Spectroscopy – III. Applications

Dave Kilkenny

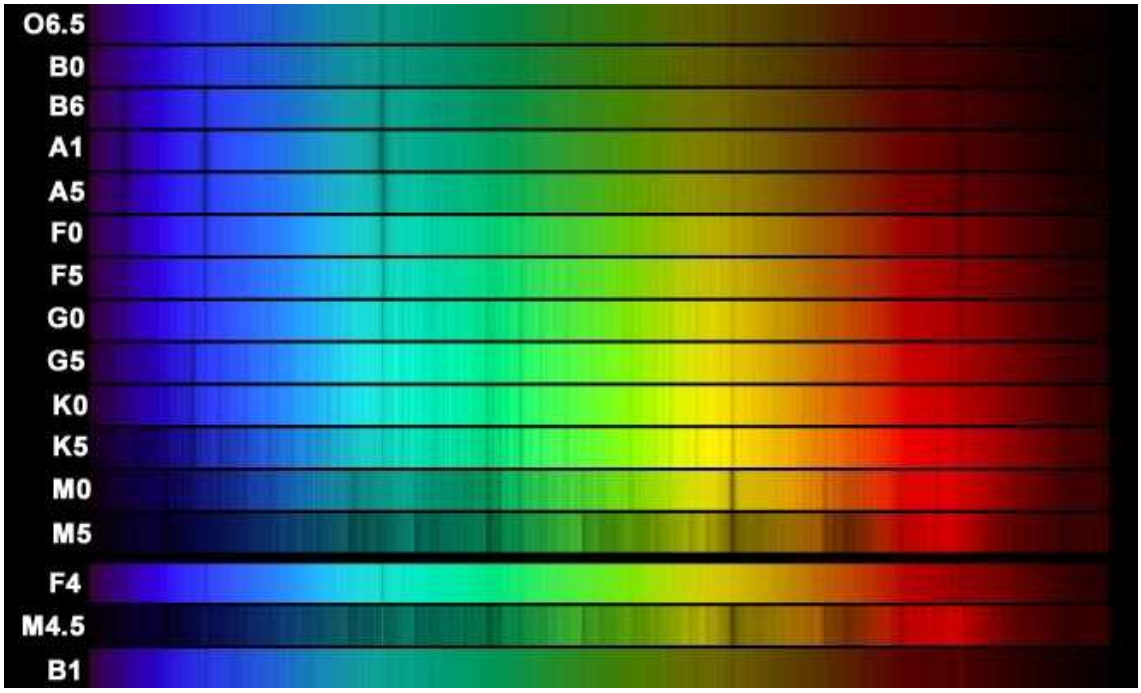

Contents

1 Spectral types

The classification of spectra – just by looking at them – is sometimes dismissed as "butterfly collecting", but performs useful functions:

1.1 Crude classification

An objective-prism on a Schmidt telescope can obtain hundreds, possibly thousands of low-dispersion spectra at a time. As we have seen, this can be used to pick out very easily "unusual" objects such as emission-line stars, quasars and the like for further, detailed study. Similar functions can be performed photometrically (the Sloan Digital Sky Survey is an excellent example of this) – though what these are doing is effectively **very** low dispersion spectroscopy.

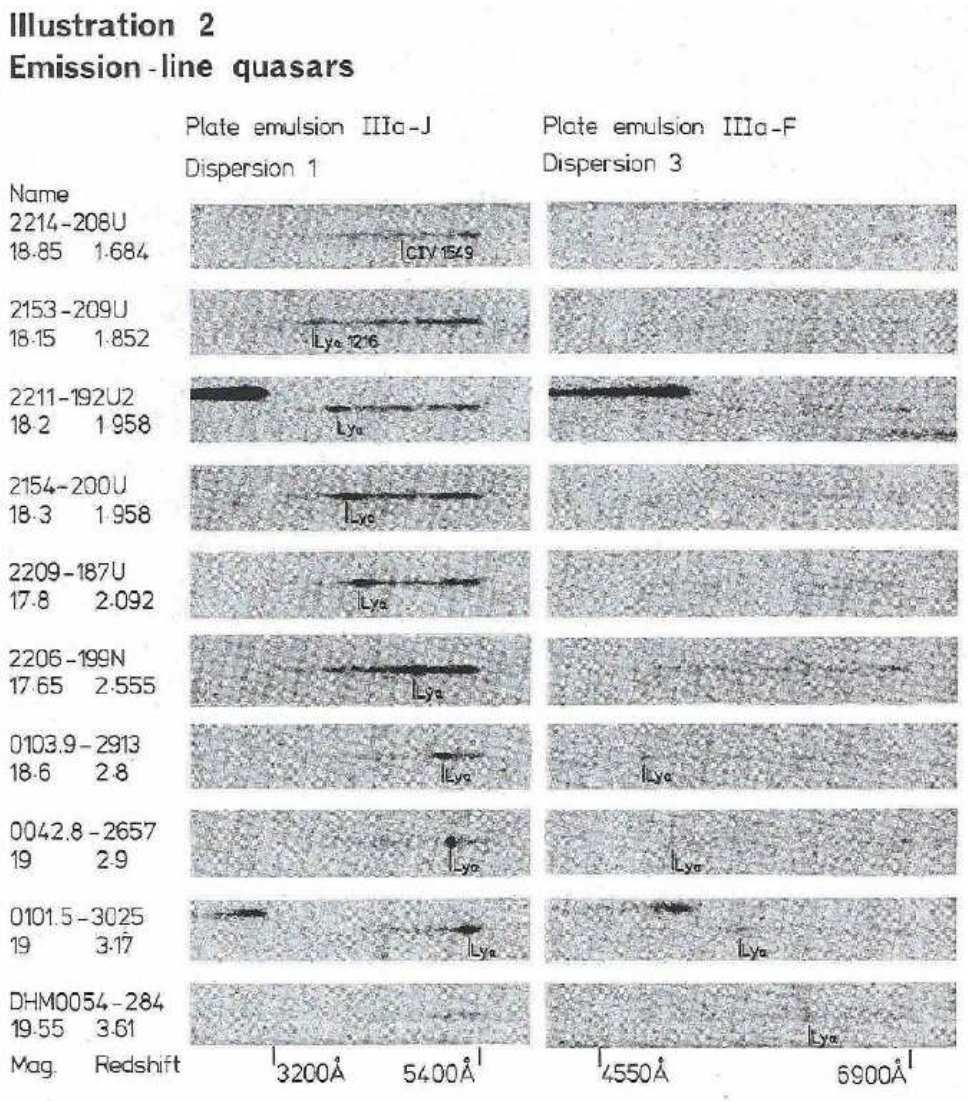

Figure 1: Emission-line quasar spectra obtained with the Anglo-Australian Schmidt telescope plus objective prism.

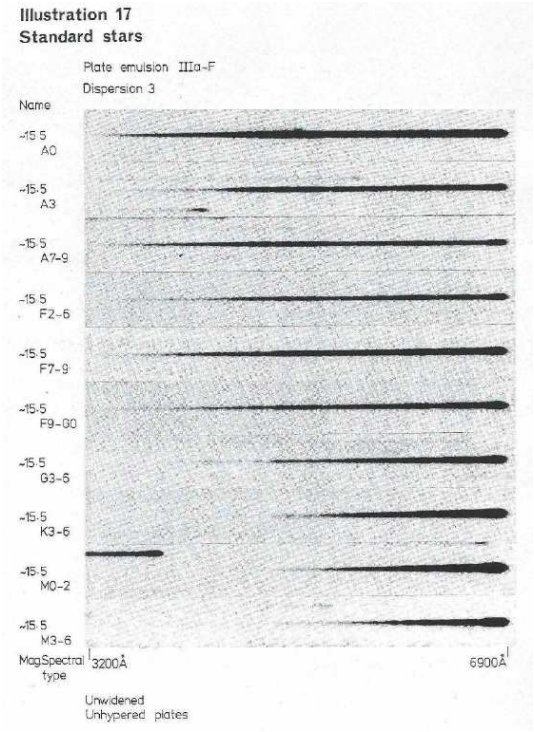

Figure 2: Unwidened spectra of "standard" stars with the AAO Schmidt.

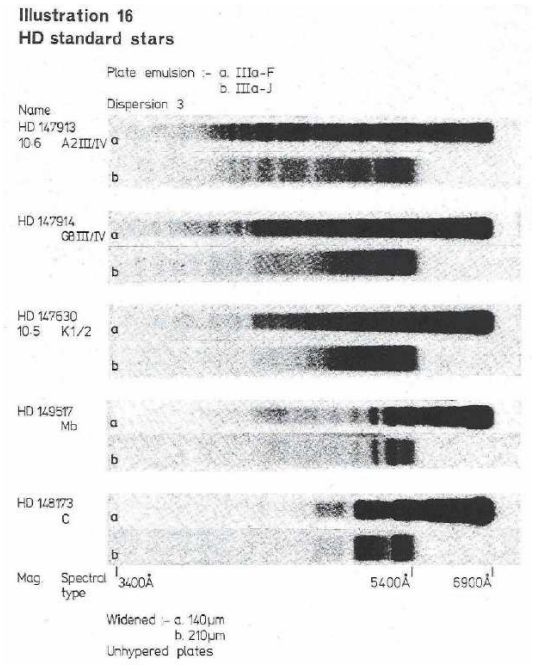

Figure 3: Widened spectra of "standard" stars with the AAO Schmidt. Note the much more obvious spectral features in th widened spectra.

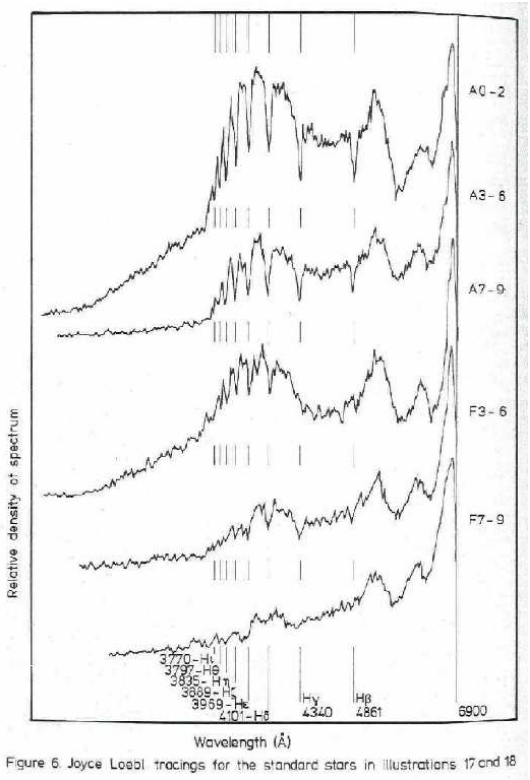

Figure 6. Joyce Loebl tracings for the standard stars in illustrations 17 and 18

Figure 4: Digitised scans of objective-prism specta.

1.2 Finer classification

We have looked at spectral typing – actually spectrum/luminosity typing – and seen that we can classify stars relatively easily into a simple sequence:

O B A F G K M

to which we should add the L and T stars – and which has been "decimalised" to give finer resolution.

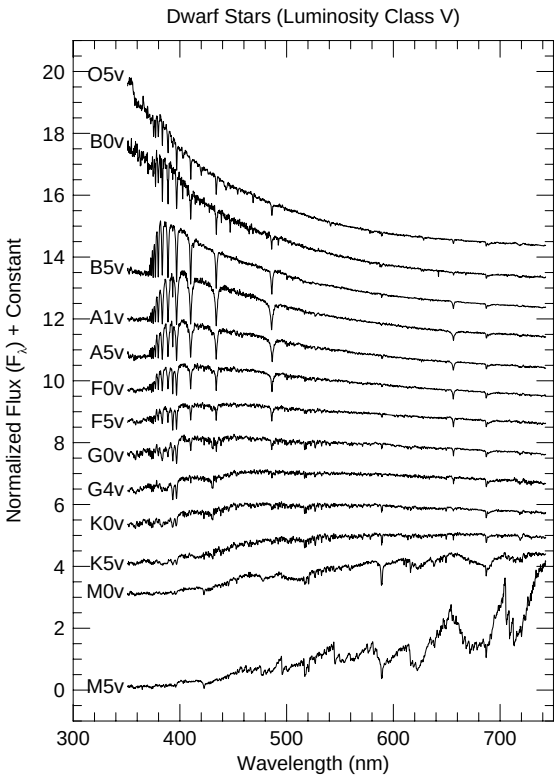

Figure 5: Sample spectral types in digital form, displayed in flux units.

We have also seen that two effects allow us to assign luminosity types to stars (I,II,...etc) based on:

- **pressure broadening** or **Stark effect** which is particularly strong for Hydrogen and Helium lines and which results in the denser atmospheres (caused by greater pressure, caused by higher surface gravity) producing broader lines and
- for elements which are partially ionised, the gas density can have a significant effect on the overall degree of ionisation. Comparison of the strengths of lines from ionised and neutral (or doubly-ionised and singly-ionised, etc) atoms of the same element can be luminosity criteria.

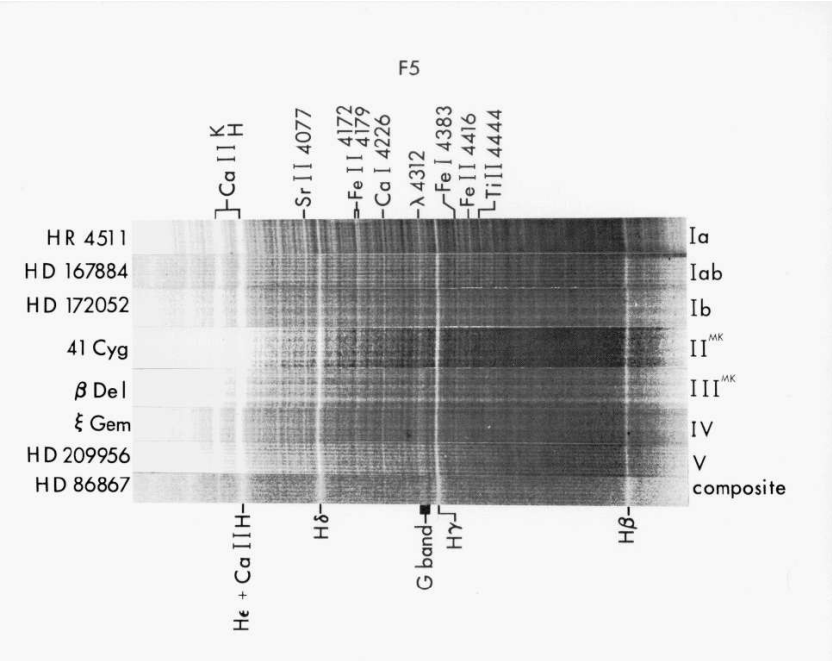

Figure 6: Objective-prism type spectra: luminosity effects at F5. Useful luminosity criteria are the lines SrII (4077Å) and FeII/TiII (4172-78Å), for example.

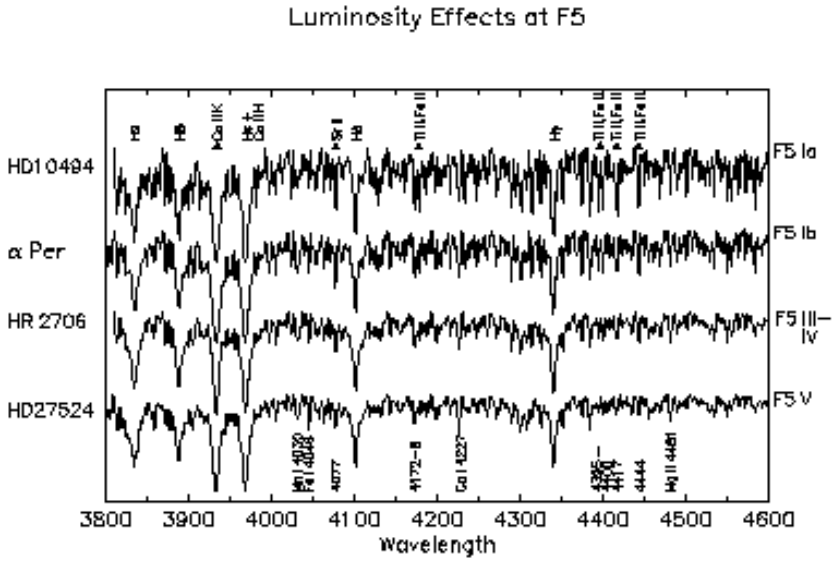

Figure 7: Digital spectra: luminosity effects at F5.

We have then, that:

$$\text{Spectral Type} \;=\; f(\text{temperature})$$

$$\text{Luminosity Type} \;=\; f(\text{surface gravity})$$

The important thing is that MK types can be calibrated against temperature and luminosity (absolute magnitude) giving us a way of determining stellar distances. Stellar radii can also be inferred from the MK types. Note that, in the Table below, which gives a calibration for MK type in terms of temperature (T_{eff}) and luminosity (absolute magnitude, M_V), temperature and luminosity are not entirely independent. One can see that the temperature at a particular spectral type might be somewhat dependent on luminosity, for example.

Table 1: An MK-type/absolute magnitude calibration (taken from "Allen's Astrophysical Quantities" Fourth Edition.

	V			III			I		
Sp type	M_V	T_{eff}	BC	M_V	T_{eff}	BC	M_V	T_{eff}	BC
05	–5.7	42000	–4.4						
09	–4.5	34000	–3.33				–6.5	32000	–3.18
B0	–4.0	30000	–3.16						
B2	–2.45	20900	–2.35				–6.4	17600	–1.58
B5	–1.2	15200	–1.46				–6.2	13600	–0.95
B8	–0.25	11400	–0.80				–6.2	11100	–0.66
A0	+0.65	9790	–0.30				–6.3	9980	–0.41
A2	+1.3	9000	–0.20				–6.5	9380	–0.28
A5	+1.95	8180	–0.15				–6.6	8610	–0.13
F0	+2.7	7300	–0.09				–6.6	7460	–0.01
F2	+3.6	7000	–0.11				–6.6	7030	–0.00
F5	+3.5	6650	–0.14				–6.6	6370	–0.03
F8	+4.0	6250	–0.16				–6.5	5750	–0.09
G0	+4.4	5940	–0.18				–6.4	5370	–0.15
G2	+4.7	5790	–0.20				–6.3	5190	–0.21
G5	+5.1	5560	–0.21	+0.9	5050	–0.34	–6.2	4930	–0.33
G8	+5.5	5310	–0.40	+0.8	4800	–0.42	–6.1	4700	–0.42
K0	+5.9	5150	–0.31	+0.7	4660	–0.50	–6.0	4550	–0.50
K2	+6.4	4830	–0.42	+0.5	4390	–0.61	–5.9	4310	–0.61
K5	+7.35	4410	–0.72	–0.2	4050	–1.02	–5.8	3990	–1.01
M0	+8.8	3840	–1.38	–0.4	3690	–1.25	–5.6	3620	–1.29
M2	+9.9	3520	–1.89	–0.6	3540	–1.62	–5.6	3370	–1.62
M5	+12.3	3170	–2.73	–0.3	3390	–2.48	–5.6	2880	–3.47

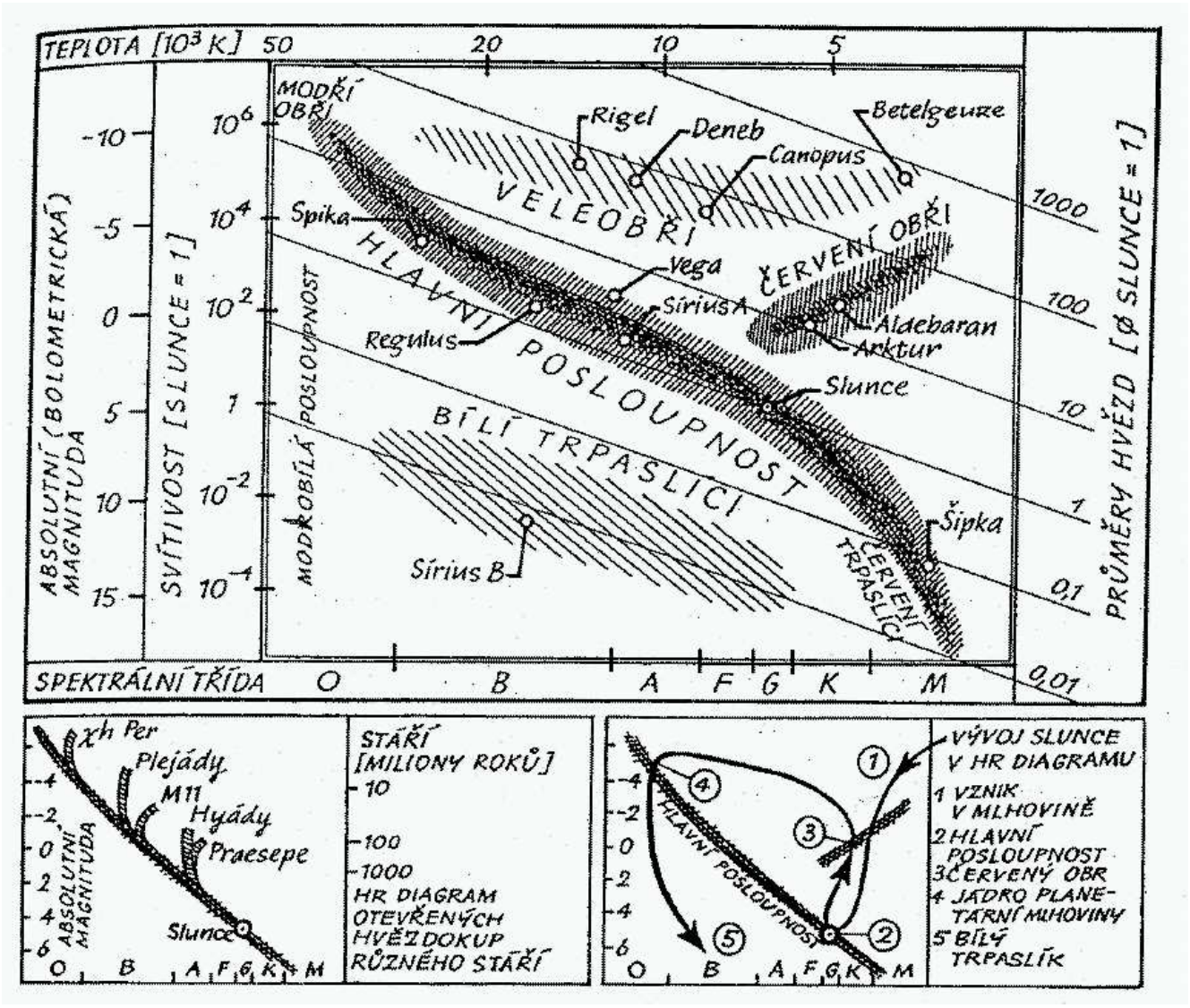

Figure 8: HR diagram with sample stars and luminosity/temperature/radius calibrations. And even though it's written in Czech, you should be able to understand it !

There follow some series of spectra from the EC survey. These are at 100 $\AA$/mm - so comparable to "classification" dispersions (the HD Catalogue was done at a variety of dispersions down to about 160 $\AA$/mm and the Michigan Spectral Catalogue at 108 $\AA$/mm at Hγ).

Although one can clearly classify stars (and other things) from such spectra, they are good enough to make quantitative velocity measurements and possibly even low grade line profile measures.

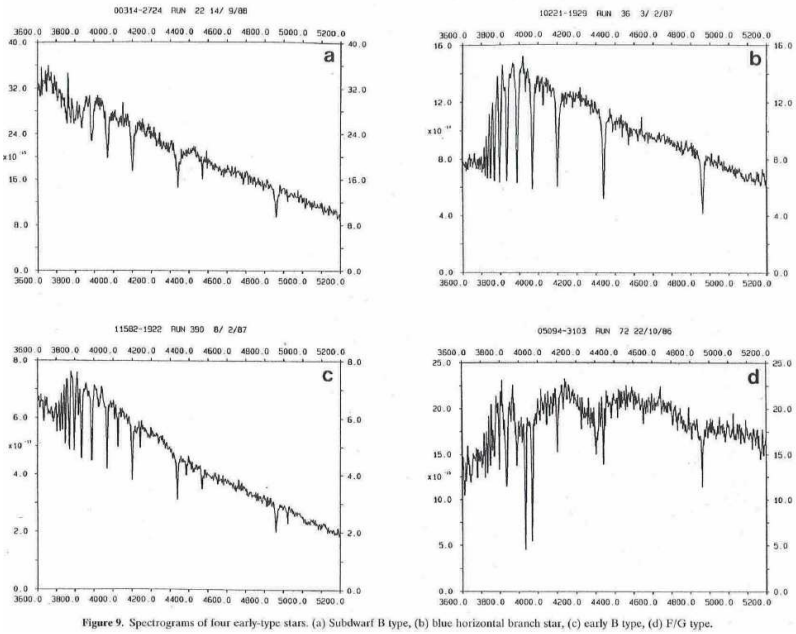

Figure 9. Spectrograms of four early-type stars. (a) Subdwarf B type, (b) blue horizontal branch star, (c) early B type, (d) F/G type.

Figure 9: EC spectrograms of "early-type" stars (a) B subdwarf, (b) blue horizontal-branch star, (c) normal mid-B star, (d) G star.

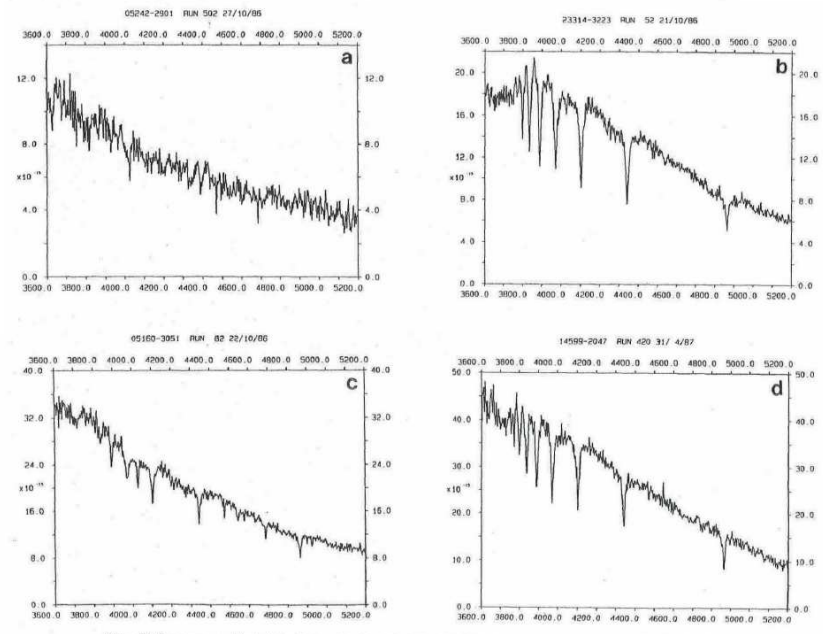

Figure 10. Spectrograms of hot subdwarf stars, all with similar $(U-B, B-V)$ colours. (a) He-sdO, (b) sdOB, (c) sdO, (d) sdB.

Figure 10: EC spectrograms of hot sudwarf stars (extended horizontal-branch) (a) Helium-rich O subdwarf, (b) sdOB, (c) sdO, (d) sdB.

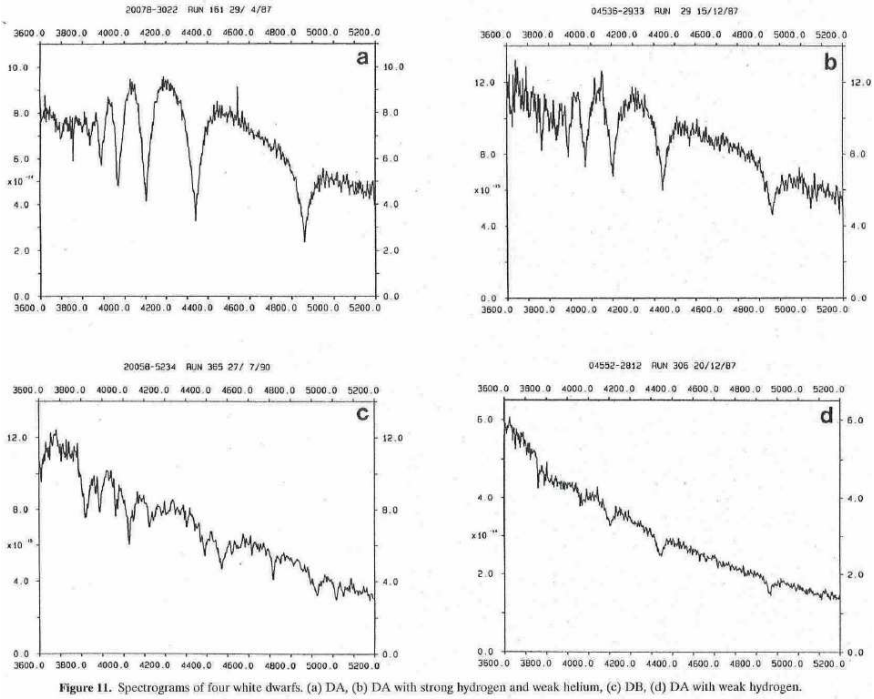

Figure 11: EC spectrograms of white dwarf stars (a) DA, (b) DA with weak He I, (c) DB, (d) DA with weak Hydrogen.

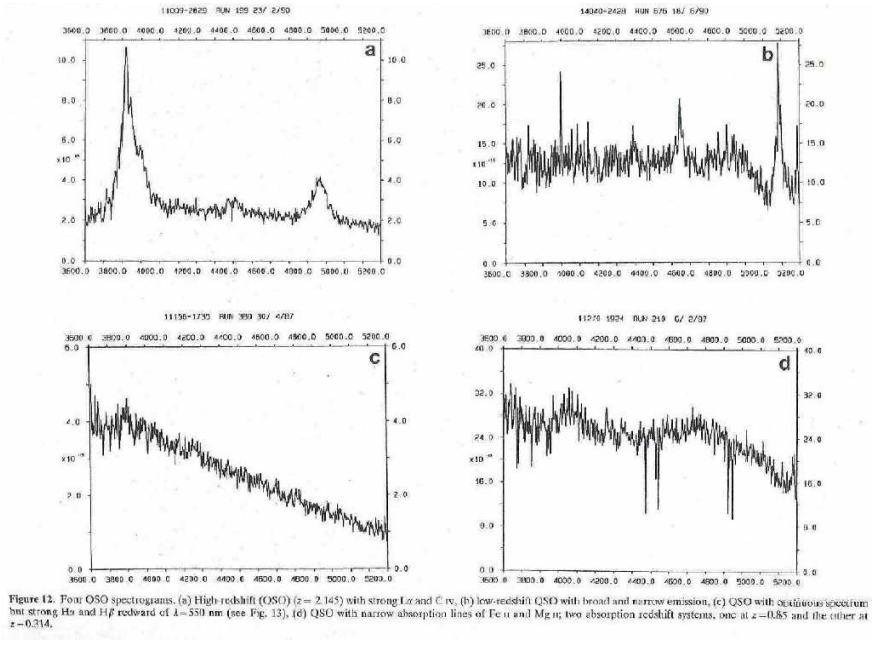

Figure 12: EC spectrograms of QSOs (Quasi-stellar objects) (a) Relatively high-redshift QSO (z=2.145), (b) Low redshift QSO with broad and narrow emission, (c) QSO with "continuous" spectrum (but strong Hα and Hβ redshifted beyond λ = 550nm, (d) QSO with narrow absorption lines of Fe II and Mg II, showing redshifts of z = 0.865 and 0.314 – due to intergalactic material.

2 Radial Velocities

We have seen previously that the radial (line-of-sight) velocity can be found by measuring the Doppler shift of spectral features. We have:

$$\frac{\Delta\lambda}{\lambda_{rest}} = \frac{\lambda_{obs} - \lambda_{rest}}{\lambda_{rest}} = \frac{v_r}{c}$$

Figure 13: Radial velocity.

which has many applications, from galaxy redshifts, galactic and cluster dynamics to binary systems and pulsating stars.

One could measure the mid point of a spectral absorption or emission line (or many lines) and use the the Doppler formula (above) to obtain a mean radial velocity. In practice, it is usual to use some kind of **cross correlation** software. What this does is to compare the spectrogram with a **"template"**, effectively multiplying them together, then shifting the spectrum by a small $\Delta\lambda$ and doing it again, and so on. A cross-correlation function is created which has a peak when the lines in the spectrogram match the lines in the template.

Cross-correlation has the advantage that it uses all the lines in the spectral region observed – and many of these might be too weak to see or lost in the "noise". It also gives an objective measurement.

2.1 Binary stars

We have looked at binary stars and the importance of double-lined systems for the determination of stellar masses. The figures below are from work by Rucinski & Lu, and show the results of cross-correlation (CCF = cross-correlation function; BF = "broadening function") in determining accurate radial velocities.

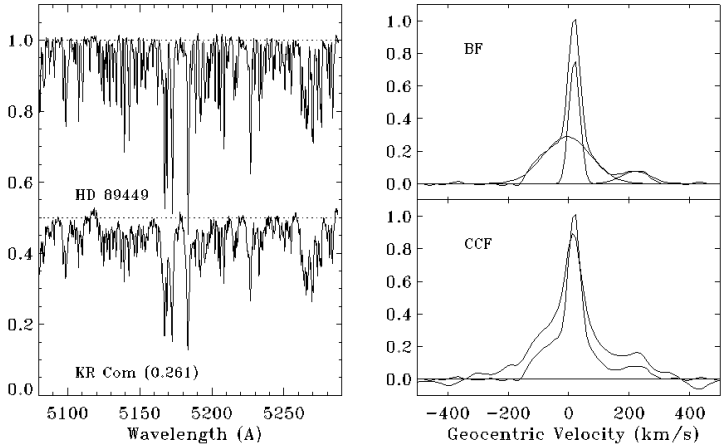

Figure 14: Cross correlation function.

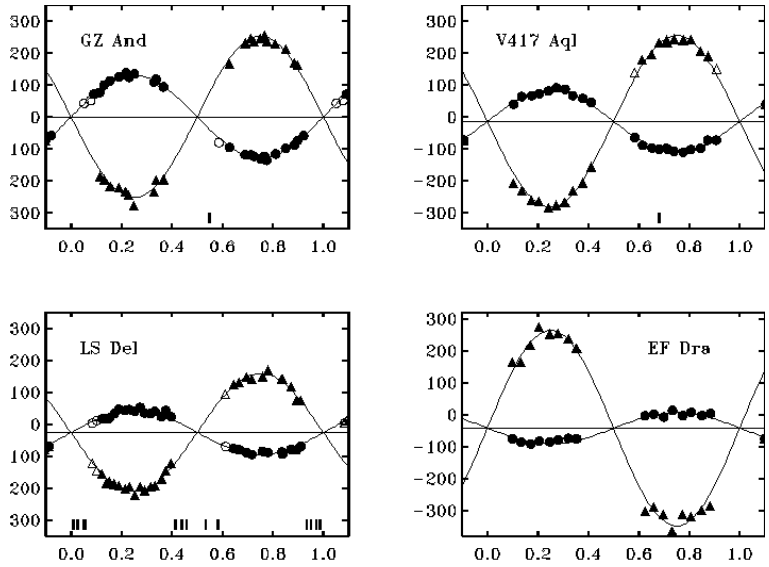

Figure 15: Velocity curves for double-lined spectroscopic binaries.

2.2 Pulsating stars

In a previous lecture (Photometry - II), we looked briefly at the light curves of two pulsating hydrogen–deficient stars and we can now re-examine these in the light of the velocity data.

The light curves are repeated below and show for both stars a light maximum at zero phase (in fact, this was how zero phase was *defined*).

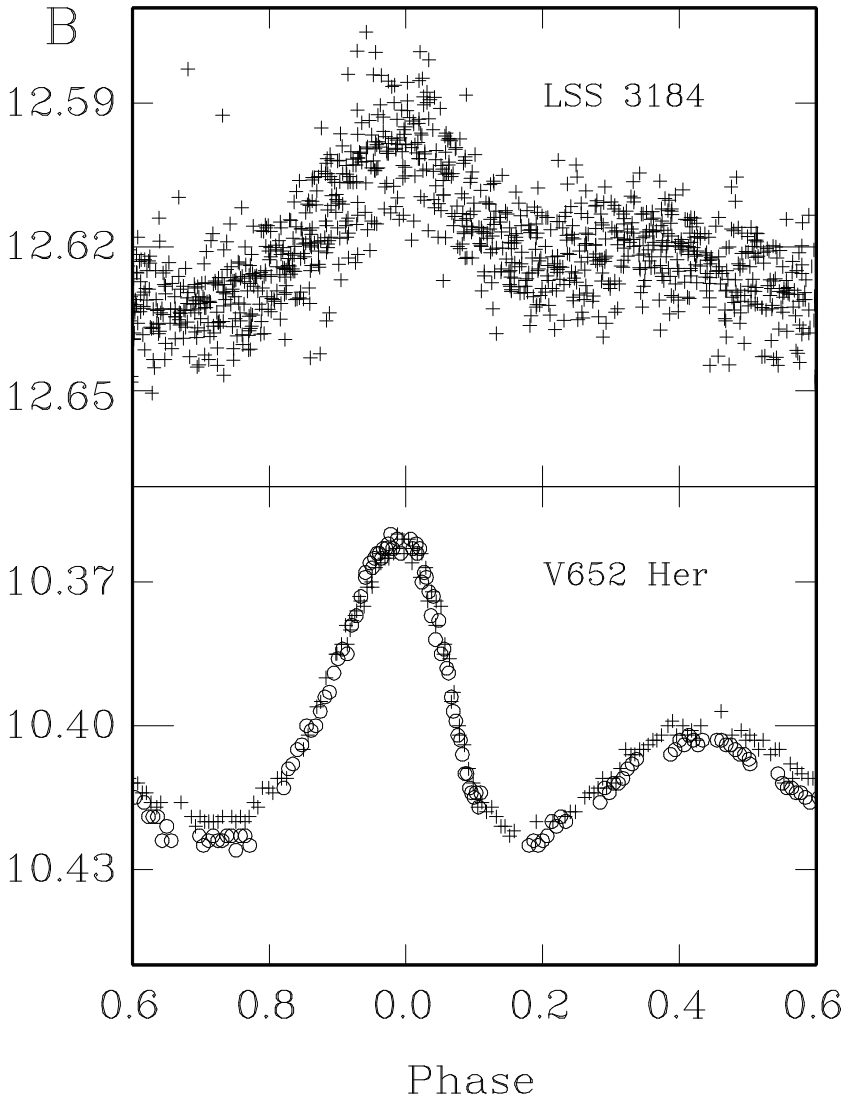

Figure 16: Phased light curves for two hydrogen-deficient stars, LSS 3184 (BX Cir) and V652 Her. (Pulsation periods for both stars ~ 0.1 day).

If we now look at the velocity curve for V652 Her (or LSS 3184), we see that the maximum positive velocity (stellar surface moving away from the observer) is just after phase zero and then undergoes a very rapid change from maximum positive velocity to maximum negative velocity – the star has reached minimum radius and "bounced", starting to expand again. The outward velocity slowly decreases to zero near phase 0.6 at which point the star is at maximum radius.

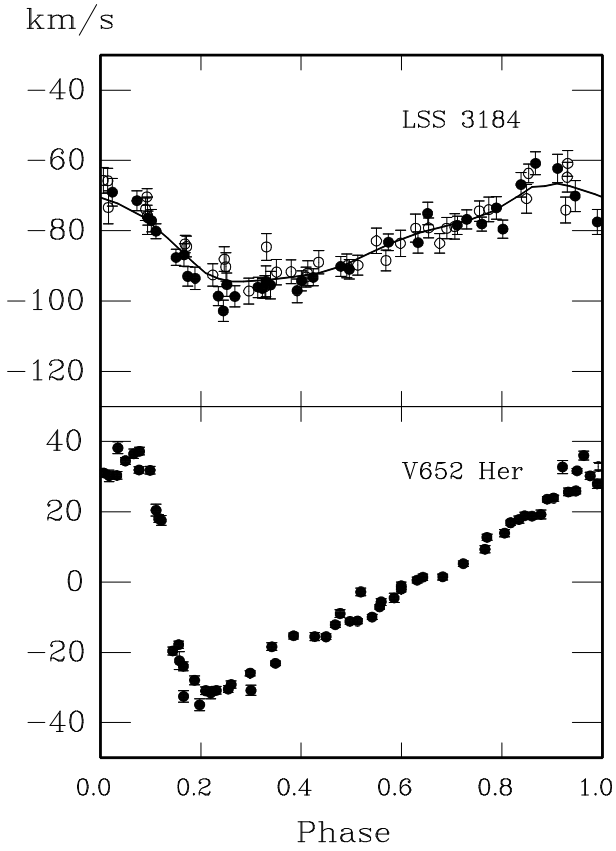

Figure 17: Radial velocity curves for the same stars, phased on the photometric period.

Recall that:

$$\text{Luminosity} \propto R^2 T^4$$

The star is at minimum radius when near maximum brightness and therefore near maximum temperature. There are two factors which generate the variation in the light curve – the temperature (T^4) and the radius (R^2) and maximum radius and maximum temperature are separated in phase by about 0.5. This explains the secondary maximum on the light curve.

Note that:

- From these data, we can infer that the stars are radial pulsators (and, in fact, they appear to be fundamental mode pulsators).
- We can therefore use the Baade-Wesselink method (or something similar) to determine the radii and luminosities of the stars.
- The velocity curve of LSS 3184 is a little gentler than that of V652 Her, but the general principles are the same.
- The mean velocity of V652 Her is near zero – it's not moving towards or away from the Sun, whereas LSS 3184 has an approach velocity near -85 km/s.

2.3 Redshifts

We can also measure the radial velocities of galaxies external to our own.

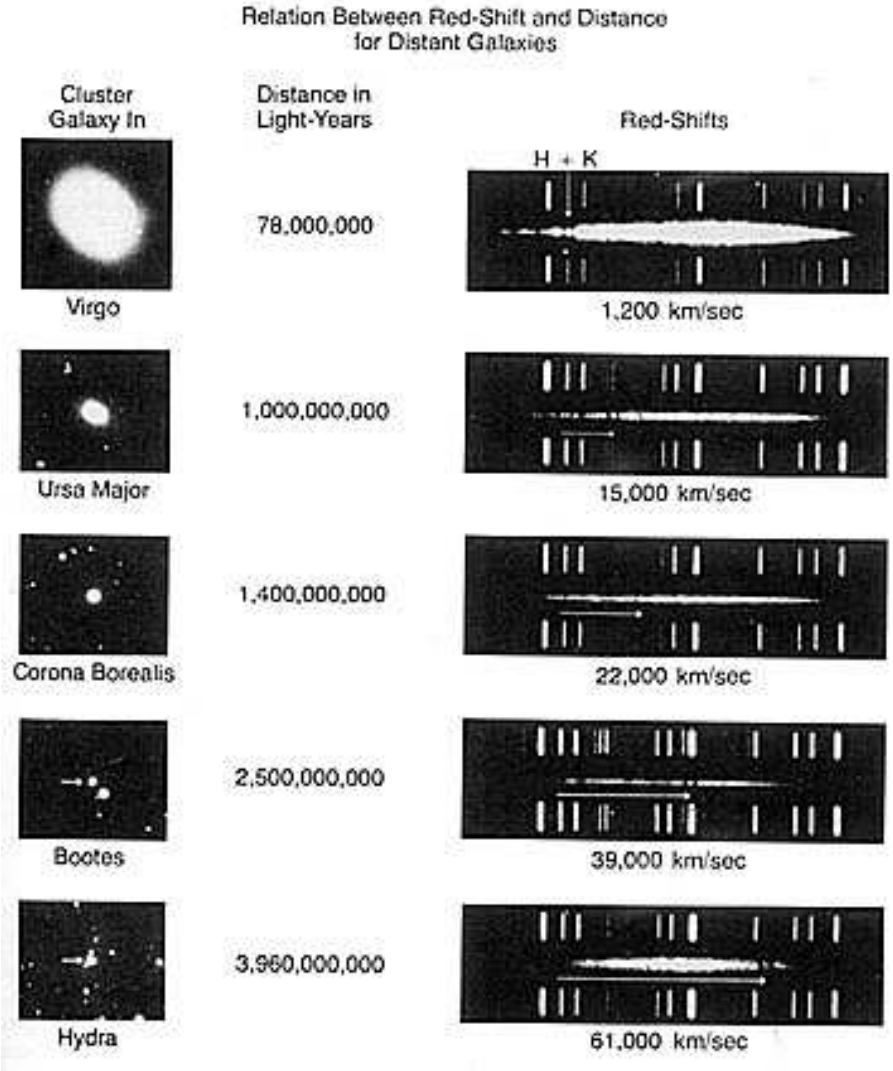

Figure 18: Old panel (used as a "laboratory exercise" when I was a kid) showing direct photgraphs and spectra for some relatively nearby galaxies. The "redshift" of the Ca II lines at (rest wavelengths of) 3933$\mathring{A}$ and 3968$\mathring{A}$ can be clearly seen. With redshifts this big, you can just about measure them with a ruler (as we did in the lab exercise) and get decent results

Measurements of galaxy velocities started with Slipher around 1914 and resulted in Hubble formulating **Hubble's Law** in 1929, which states that (for distant galaxies):

$$\text{Velocity} \quad = \quad \text{H}_0 \ \times \ \text{Distance}$$

where H_0 is **Hubble's constant** (at the present) and is currently determined to be about 70 km/sec/Megaparsec. That is, **on average** galaxies at a distance of 10 Mpc will be receding at 700 km/sec, galaxies at 100 Mpc will be receding at 7000 km/sec, and so on.

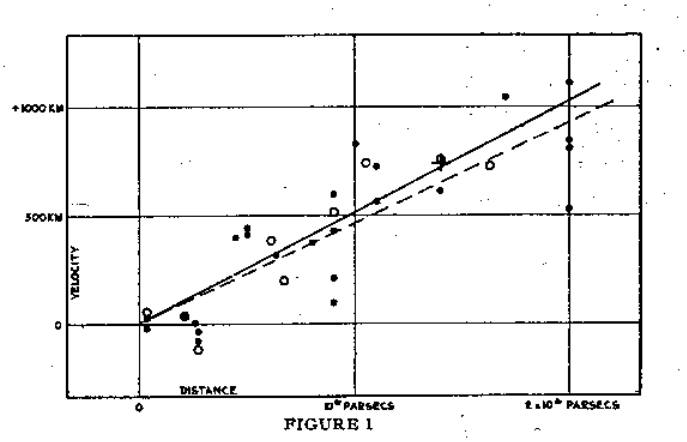

Figure 19: Hubble's original "redshift" diagram (1929).

In dealing with galaxies/cosmology, z is usually used as the velocity indicator where:

$$z \;=\; \frac{\lambda_{observed} \;-\; \lambda_{rest}}{\lambda_{rest}} \;=\; \frac{\Delta\lambda}{\lambda_{rest}}$$

Note that we cannot now write $\Delta\lambda/\lambda = v/c$ because relativistic effects become important as v gets nearer to c and:

$$z \;=\; \frac{\Delta\,\lambda}{\lambda} \;=\; \sqrt{\frac{(1\;+\;v/c)}{(1\;-\;v/c)}} \;-\; 1$$

where v is the velocity of the source. Now z can take any positive value (for a "redshift") and we have seen that the SDSS has found quasars with $z > 6$ (and note that, using the above equation, a quasar with a redshift $z = 6$ is motoring along at 96% of the speed of light ....

Of course, it is easy to see how the velocity/redshift of a distant object can be measured from spectral line shifts (though at high z, **identifying** the lines in not always trivial). But how does one determine the distance ??

We have seen in previous lectures how a systematic distance "ladder" can be built up. Briefly:

- For the nearest stars, we can use the **parallax** to get distance and thus luminosity.
- By establishing luminosities for nearby stars of known **MK type**, we can determine the distances of nearby clusters containing more luminous stars.
- And by **main-sequence fitting** of cluster **colour-magnitude diagrams** we can calibrate more distant clusters, obtaining luminosities for Cepheid (and other) variables.
- With a **zero-point** for Cepheids, we can use the Cepheid **Period-Luminosity relation** to determine the distances of at least nearby galaxies.

It's not as simple as that, of course; interstellar reddening effects (for example) can introduce uncertainties. But say we can do it, what about really distant objects ??

It was initially assumed that we could use the (supposedly linear) Hubble Law – once calibrated – to get the distances of really distant objects. Now, the exact shape of the Velocity–Distance

relation is critical to determining the nature of the Universe, and so determining this requires independent distance measurement.
A number of "indirect" methods have been found to determine distances of more distant galaxies:

2.3.1 The Tully-Fisher relation

Very briefly, this works because the more massive a galaxy is, the faster it will rotate. And because there is a relationship between the mass of a galaxy and the light it emits (the **mass-to-light ratio**) it is possible to derive a relation betweeen the rotation speed and luminosity:

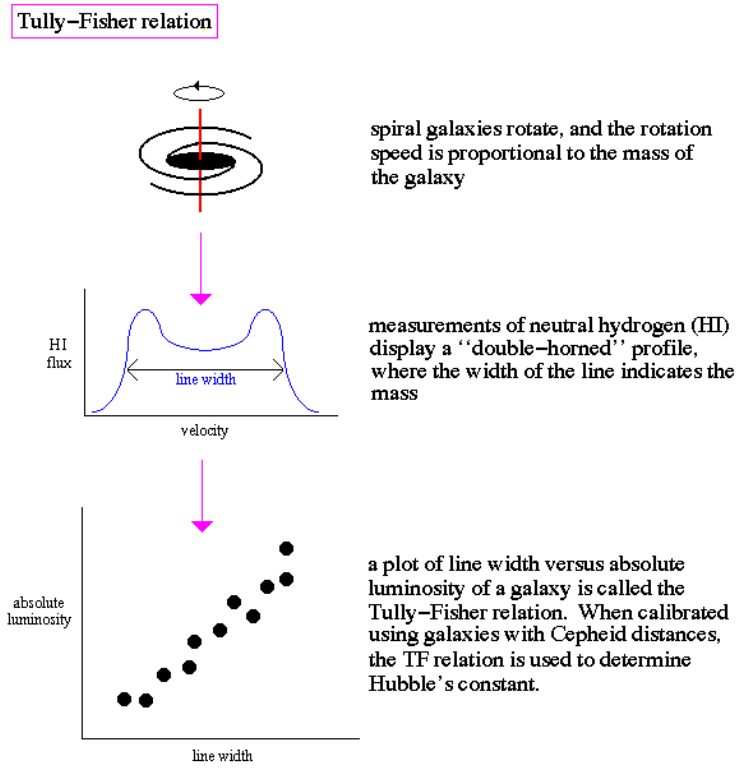

Figure 20: Schematic of the Tully-Fisher relation.

That the Tully-Fisher relation works at all is somewhat surprising. It depends on three fundamental ideas:

- That galaxies must be circularly symmetric (so you can correct for inclination ($sin\ i$) effects). This is not such a bad assumption for spiral galaxies.
- That all galaxies (of some type) have the same mass/luminosity relation. This is not true.
- That all galaxies have the same surface brightness. This is even more untrue – there even exists a class "Low Surface Brightness" (LSB) galaxies – with the inevitable three letter acronym (TLA).

In spite of the above, and with some precautions, a relation can be established, and is used for distance-determination:

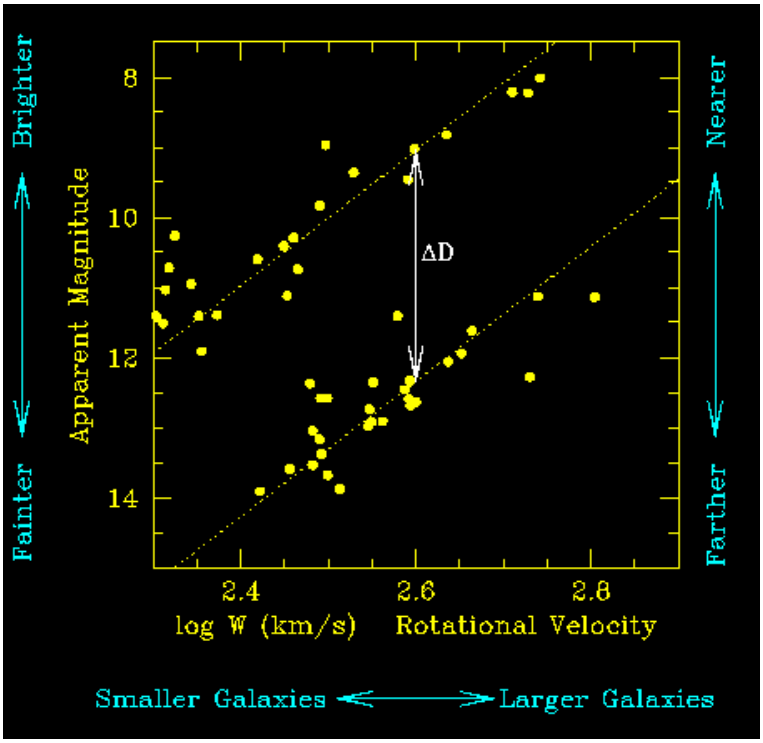

Figure 21: Tully-Fisher relation for two clusters of galaxies. The vertical difference gives the relative distance/luminosity.

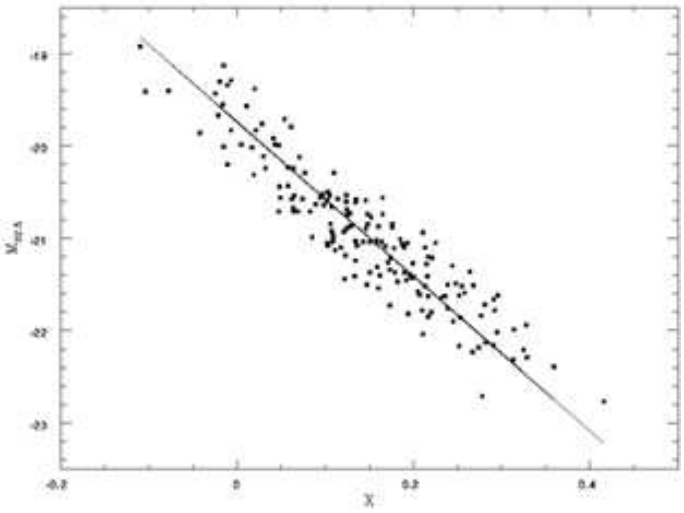

Figure 22: The Tully-Fisher relation between rotational velocity and I-band luminosity for a large sample of spiral galaxies (Dell'Antonio et al. 1996). Of course, before you can make a plot such as the above, you have to know the luminosities of the galaxies – you have to be able to calibrate the system. This can be done, for example, if you have Cepheids in a galaxy – if that galaxy is in a cluster, you have then a much bigger sample for the calibration.

2.3.2 Type Ia supernovae

Type II supernovae are massive, evolved stars which run out of nuclear fuel and collapse, followed by a massive explosion. Such explosions might have quite different luminosities.

Figure 23: Before (right) and after (left) photographs of SN1987a. The right hand plate is a good example of "archive" material; probably one of the only times the precursor to a supernova has been identified.

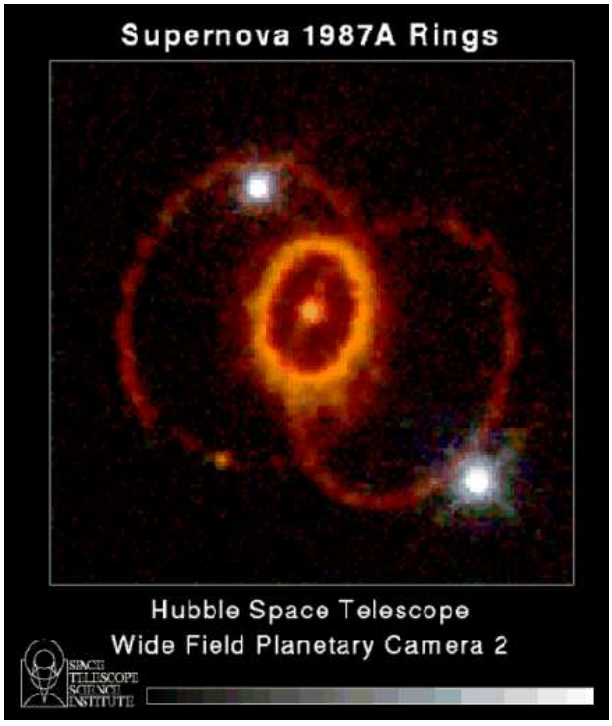

Figure 24: SN1987a in 1994.

Type Ia supernovae, by contrast, are explosions of degenerate white dwarf stars which are presumably pushed over the Chandrasekhar limit by accreting material from a companion star – or they might be a result of white dwarf mergers – which is much the same thing.

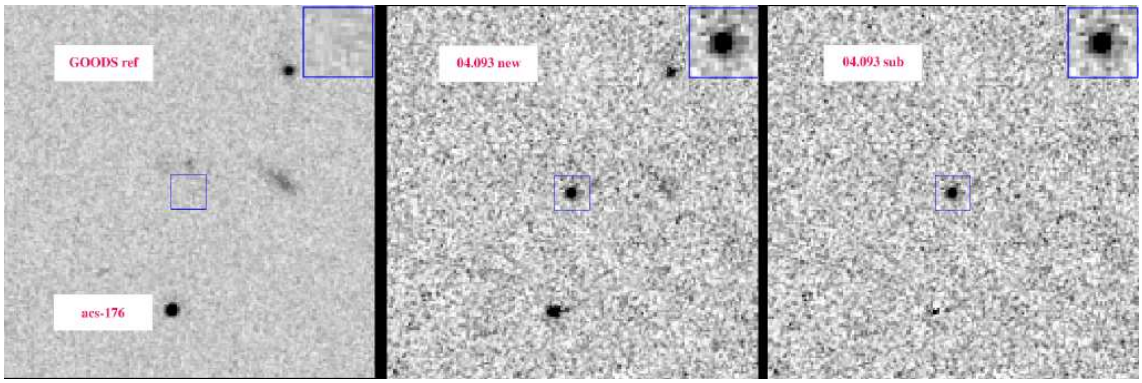

Figure 25: Very distant supernova from the **Supernova Cosmology Project**. The web page for the SCP is well worth a look at *panisse.lbl.gov*

It is known that type Ia supernova do not have the same luminosity, but it turns out that corrections for this can be made using the shape of the decline in light after the explosion.

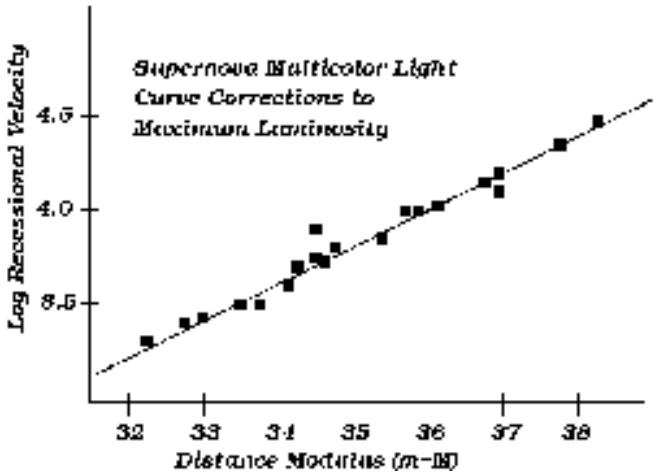

Figure 26: Hubble diagram produced using type Ia supernovae

Corrections based on multi-colour light curves appear to work well – see figure below – but there are also reasons to treat this method with care.

- The supernova must be detected quickly to determine "peak" brightness, as the rise time is short (it's an explosion, after all).
- Interstellar (intergalactic) reddening estimates can be tricky. There's not much material, but the path length is long. "Local" material (near the supernova) can confuse things.

- It is by no means clear that we understand what is happening well enough to believe these objects are real "standard candles".

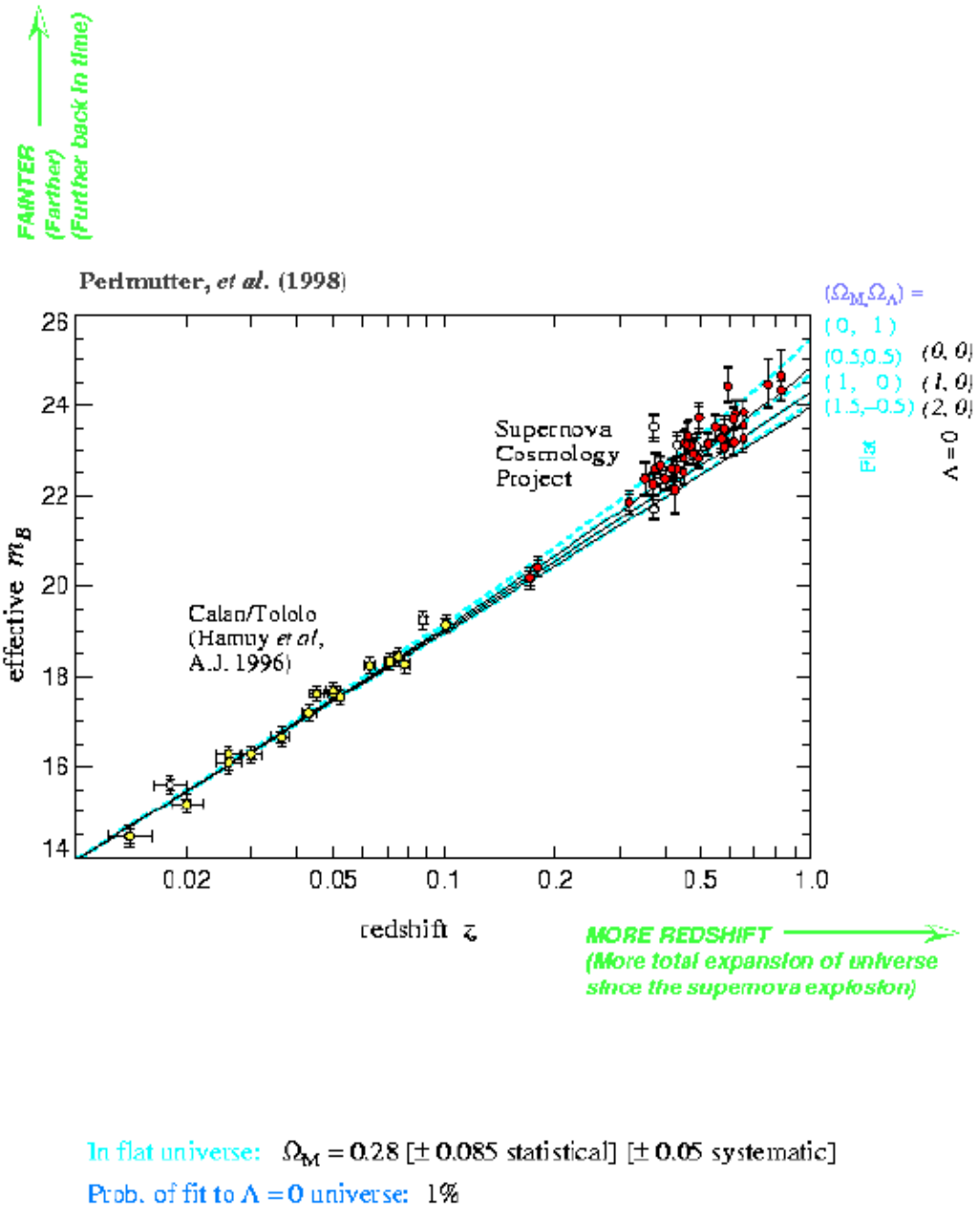

Figure 27: Type Ia supernova results; testing the Universe.

2.4 Exoplanets

The search for planets orbiting other stars ("exoplanets") has required extraordinary care in various ways:

- Ensuring that the spectrograph is extremely accurate and stable.
- Using novel data acquisition and reduction techniques.
- Paying particular care to correcting data for solar system effects.

In the case of the last item, this means (for example) taking great care in correcting to the barycentre of the solar system. Jupiter has an effect on the Sun with an amplitude of 12.4 m/sec; Saturn affects the Sun with an amplitude of 2.7 m/sec - for much stellar and galactic work, these effects can usually be ignored, but not when searching for the tiny effects that planets orbiting other stars would cause.

One exoplanet group led by Marcy & Butler (see the excellent web page *exoplanets.org*) use an echelle spectrograph which acquires the entire visible and near infrared spectrum at a resolution, R = 62000.

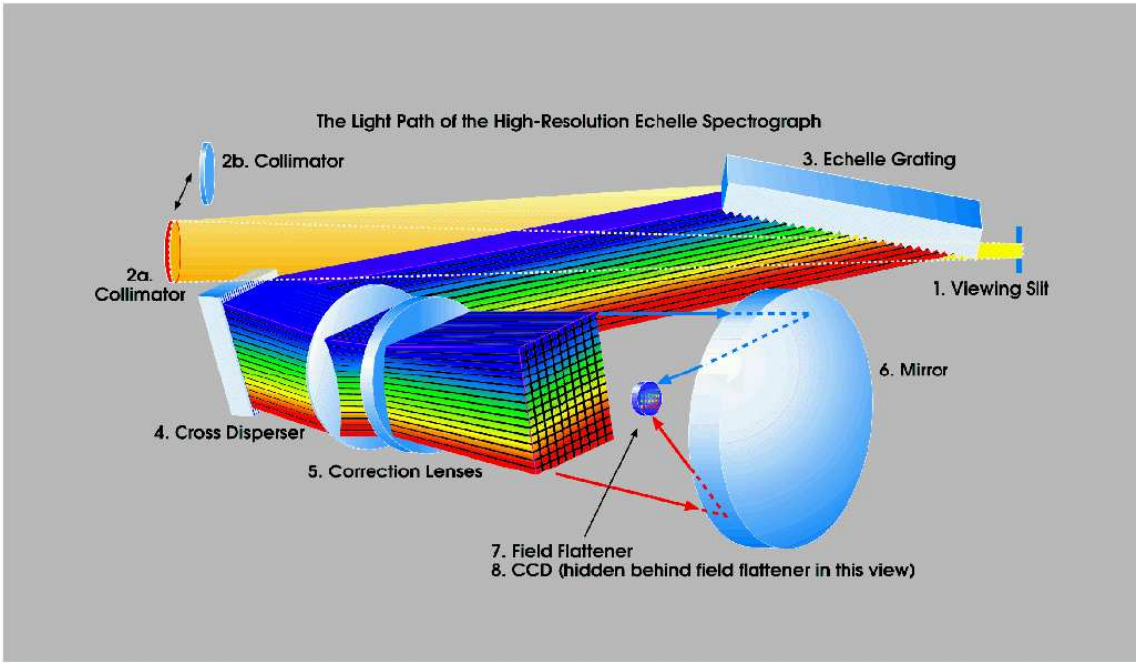

Figure 28: Schematic for the high resolution spectrograph on the Keck telescope.

Unconventionally, but of vital importance, rather than acquire the comparison arcs before and after the stellar spectrum, a comparison iodine spectrum is actually superimposed on the stellar spectrum. This requires that each spectrum (star + iodine) be modelled – one of the parameters that results from the modelling is the stellar radial velocity, and it has proved possible to attain accuracies of 3 m/sec given a S/N $\sim$ 200. This generally means using fairly big telescopes on relatively bright stars – and, of course, a lot of telescope time is needed so that stars can be followed for long and relatively continuous periods.

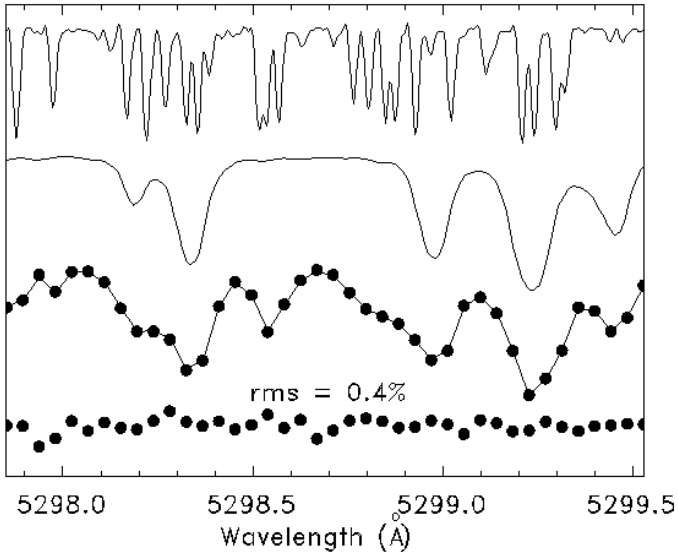

Figure 29: Top – template iodine spectrum; Second – Template spectrum for τ Ceti; Third – points are an observation of τ Ceti (+ iodine) and the line is the model; Bottom – 10 times the difference between model and observations.

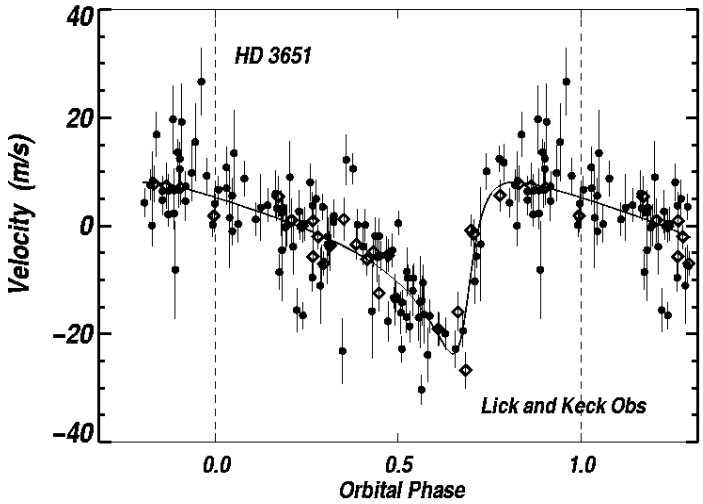

Figure 30: Recently discovered variation in radial velocity of the KOV star, HD3651. The period, $P = 62.23 day$; eccentricity, $e = 0.63$; velocity amplitude, $K = 15.9 m/s$; semi-major axis, $a = 0.284 AU$; and the derived $M\ sin\ i = 0.2\ M_J$ – about the size of Saturn.

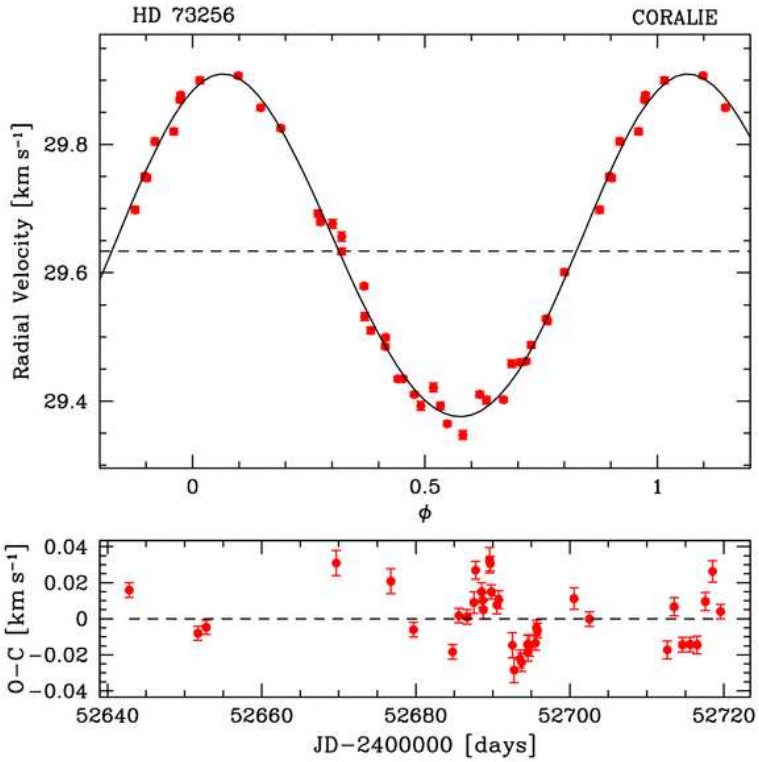

Figure 31: Recently discovered variation in radial velocity of the G8/KO star, HD73256. $P = 2.54858 day$; $e = 0.029$; $K = 269 m/s$; $a = 0.037 AU$; $M\ sin\ i = 1.87\ M_J$.

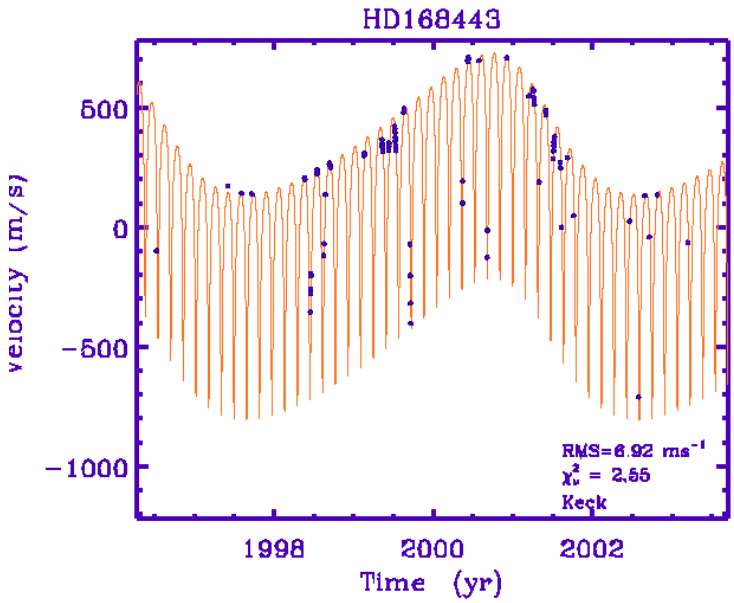

Figure 32: Two planets orbiting the G5IV star, HD168443. $P_1 = 58.10 day$; $e_1 = 0.53$; $K_1 = 472.7 m/s$; $a_1 = 0.295 AU$; $M_1\ sin\ i_1 = 7.73\ M_J$. $P_2 = 4.85 yr$; $e_2 = 0.20$; $K_2 = 289 m/s$; $a_2 = 2.87 AU$; $M_2\ sin\ i_2 = 17.2\ M_J$

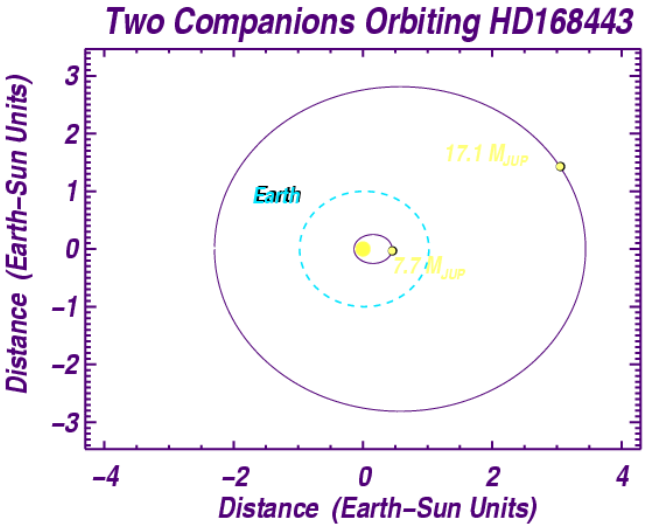

Figure 33: Representation of the HD168443 system.

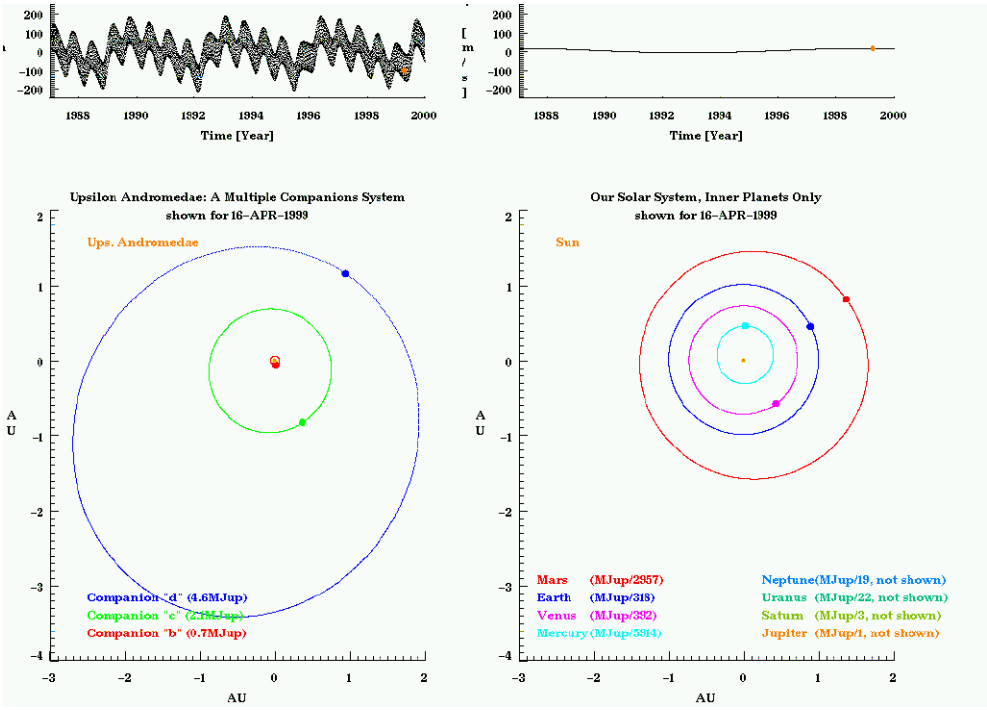

Figure 34: Representation of the three planet system υ And.

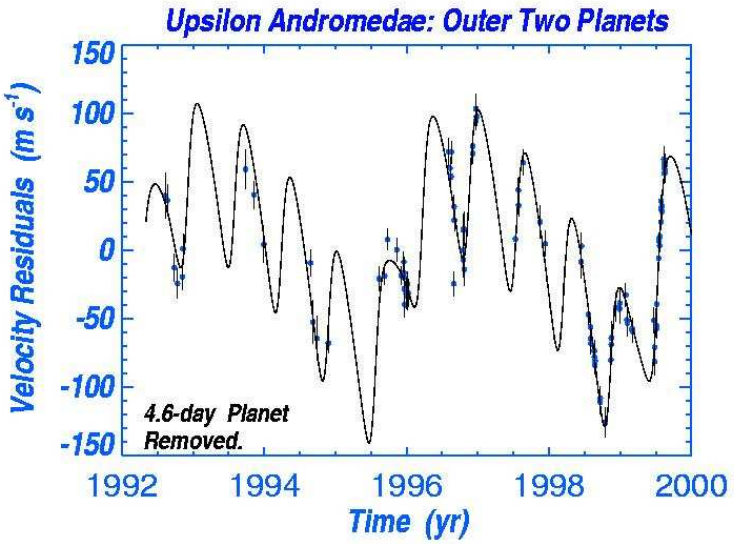

Figure 35: Actual data for υ And.

A recent very interesting result (see figure below) shows that metal-rich stars are more likely to have planets. This is not entirely surprising – if a star has no metals, you could not have Earth-like planets. But is it suggesting that to have gas giants (like Jupiter), rocky or metallic cores must first form ? A problem for you to research.

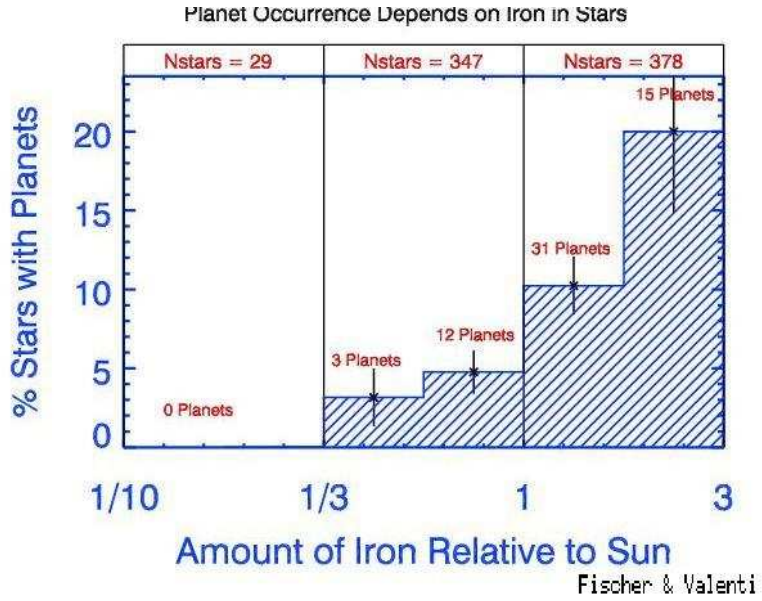

Figure 36: Recent results on atmospheric analyses of stars with planets.

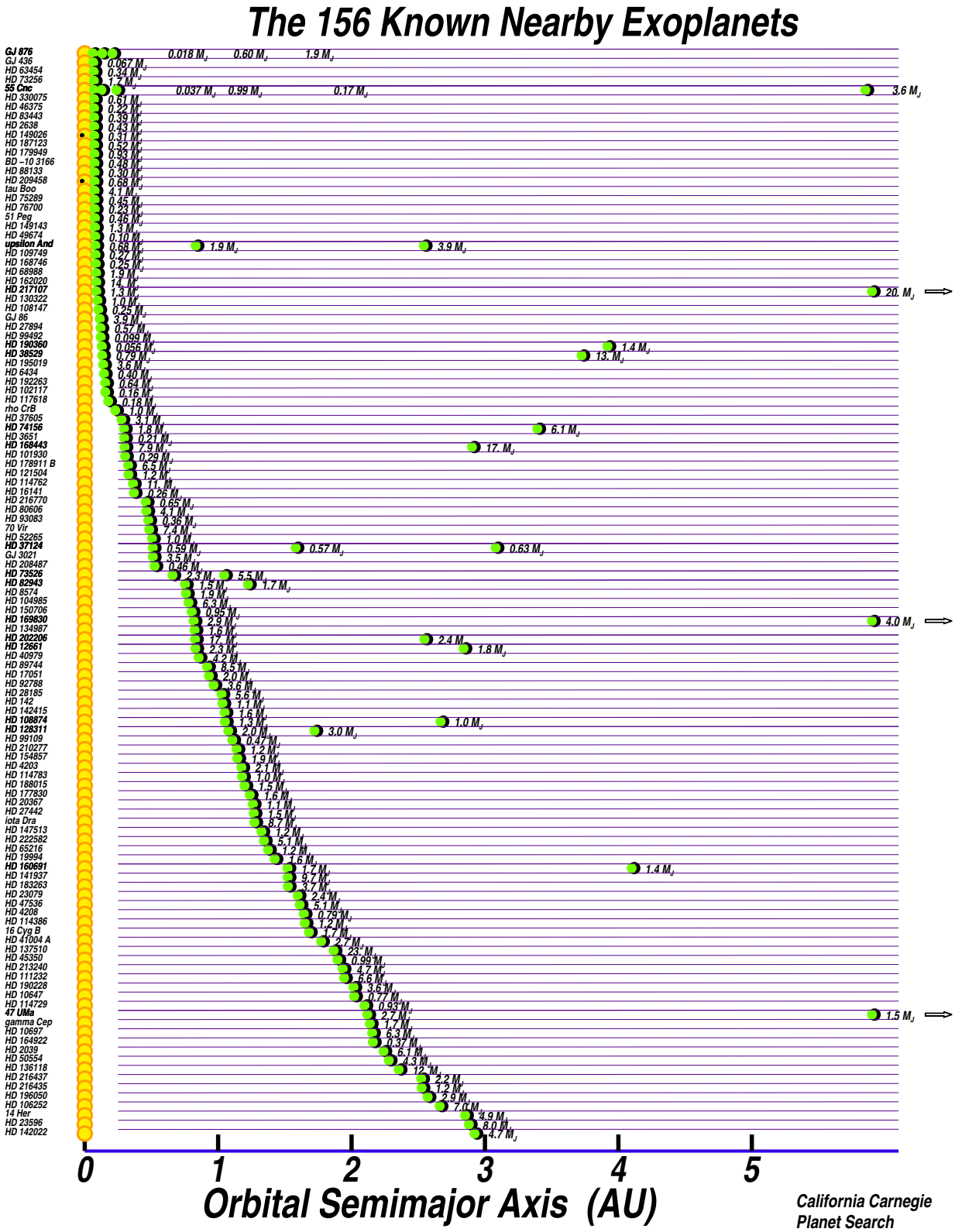

Figure 37: PLanets (outside the solar system) detected to June 2005.